High-Resolution Probing of Cellular Force Transmission

Daisuke Mizuno,[1] Rommel Bacabac,[2] Catherine Tardin,[3] David Head,[4] and Christoph F. Schmidt[5]

[1]*Organization for the Promotion of Advanced Research, Kyushu University, 812-8581, Fukuoka, Japan*
[2]*Department of Oral Cell Biology, ACTA-Vrije Universiteit, 1081 BT Amsterdam, The Netherlands*
[3]*IPBS/CNRS, 31062 Toulouse Cedex, France*
[4]*Institute of Industrial Science, University of Tokyo, Meguro-ku, Tokyo 153-8505, Japan*
[5]*III. Physikalisches Institut, Georg-August-Universität, 37077 Göttingen, Germany*

(Received 15 November 2008; published 20 April 2009)

Cells actively probe mechanical properties of their environment by exerting internally generated forces. The response they encounter profoundly affects their behavior. Here we measure in a simple geometry the forces a cell exerts suspended by two optical traps. Our assay quantifies both the overall force and the fraction of that force transmitted to the environment. Mimicking environments of varying stiffness by adjusting the strength of the traps, we found that the force transmission is highly dependent on external compliance. This suggests a calibration mechanism for cellular mechanosensing.

DOI: 10.1103/PhysRevLett.102.168102 PACS numbers: 87.17.Rt, 83.85.Ei, 87.16.dj, 87.16.dm

Cells, be they single cell organisms or part of a tissue, constantly communicate with their environment. Apart from chemical sensing, cells perform mechanosensing; they sense external forces and actively probe the environment they are embedded in [1,2]. Mechanical signals influence cell growth, development, and fate. Just like an engineer would do, cells explore external material properties by imposing a force and measuring the response. Cells generate forces by contracting their ''inner muscles,'' i.e., the *cytoskeleton*, composed largely of actin networks and bundles (stress fibers), actuated by myosin motor proteins [3]. The cytoskeleton is coupled to the external environment via specialized adhesion contacts, the focal adhesions [4,5] where cellular stress sensors are believed to be localized [6,7].

The physical and molecular details of stress sensing remain largely unknown. It has been difficult to quantify stress in cells due to their complex shapes and internal structures. The fraction of the internally generated force transmitted to the environment furthermore depends on the mechanical properties of both cell and environment, and on the geometry of adhesion. Here we present a new experimental approach that allows us to measure simultaneously the cell's viscoelastic response, the overall force the cell generates, and the fraction of this force transmitted to the environment. In the simple geometry of a spherical cell shape, suspended between two optically trapped colloids, we demonstrate how the transmitted force directly scales with the external stiffness. This result suggests a mechanism by which cells can calibrate their own active mechanosensing machinery.

The approach we use is a variation of optical-trap based microrheology (MR) which can be done actively (AMR) [8–11] or passively (PMR) by tracking fluctuations [12–14]. Both AMR and PMR can be performed with single probe particles [12,13] or pairs of probes [14–16]. We have carried out two-particle AMR and PMR (2P-AMR and 2P-PMR) simultaneously on osteocytelike MLO-Y4 cells [17] to be able to dissect nonequilibrium fluctuations generated by the cellular forces from thermal fluctuations. The latter are connected to the cell's response via the fluctuation-dissipation theorem (FDT). We tracked the motions of the probes by laser interferometry and quadrant photodiodes ($\sim$0.1 nm resolution) [18,19]. Two laser beams ($\lambda =$ 1064 nm, Nd : YVO_4, Compass, Coherent) with orthogonal polarizations created two optical traps [15]. For AMR, one particle was oscillated with an acousto-optical deflector [10]. The position signal of the other particle, relative to the center of the optical trap, was measured with a lock-in amplifier. Via trap stiffness, displacement translates to force on a particle. For PMR, the oscillation of the driving laser was turned off, and the spontaneous fluctuations in the positions of both particles were recorded. Displacements and trap stiffnesses were calibrated by recording fluctuations of one particle from the batch used in water [10,13,20]. Cells were cultured and prepared for experiments as described in Ref. [21]. Fibronectin-coated polystyrene particles (4 μm diameter) were attached to opposite sides of a cell and suspended by the optical traps [21]. Cells remained roughly spherical [Fig. 1(a)]. Experiments were carried out in a CO_2-free culture medium at 37 °C. Lipid vesicles coated with filamentous actin (F-actin) [22] were used as controls.

For 2P-AMR, the response function $A_{ij} = A'_{ij} + iA''_{ij}$ defined by $A_{ij} \equiv u_j/d_i$ was obtained by measuring the displacement u_j of particle j, caused by the force d_i on particle i, in the direction parallel to the line connecting the two particles. For 2P-PMR, the Fourier transform of the cross-correlation function of the spontaneous particle fluctuations $\langle u_i(\omega)u_j^*(\omega)\rangle \equiv \int\langle u_i(t)u_j(0)\rangle \exp(i\omega t)dt$ was calculated. In equilibrium, the fluctuation-dissipation theorem relates this function $\langle u_i u_j^*\rangle$ to the imaginary part of the complex response function A''_{ij} by

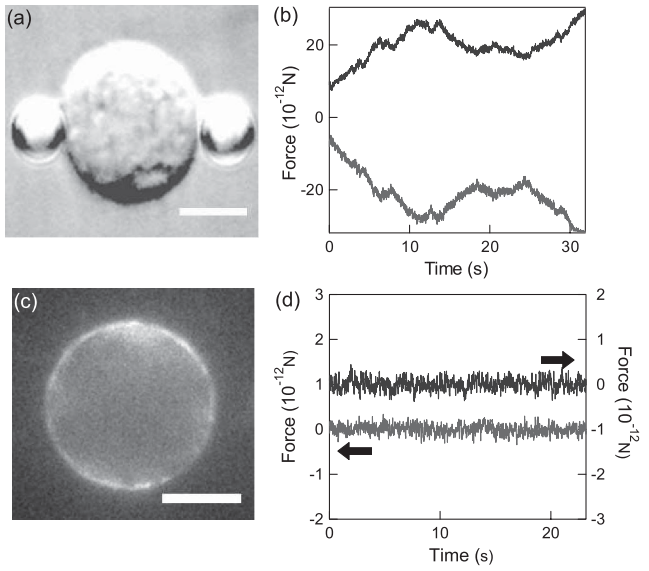

FIG. 1. (a) Differential interference contrast image of a MLO-Y4 cell suspended by two optically trapped spherical particles (polystyrene, diameter $2R = 4$ μm) attached to opposing sides of the cell. Scale bar: 5 μm. (b) Fluctuations of the force exerted on both probe particles ($k = 5.0 \times 10^{-5}$ N/m). Forces generated by the cell result in anticorrelated displacements. (c) Fluorescence image of a lipid vesicle coated with rhodamine-phalloidin stabilized and biotinylated actin. Scale bar: 5 μm. (d) Thermal force fluctuations seen by streptavidin-coated particles (spherical silica, diameter $2R = 1.5$ μm) attached via the biotinylated actin.

$$P_{\mathrm{th}}(\omega) = 2k_B T A''_{ij}/\omega. \quad (1)$$

The real part A'_{ij} is estimated through a Kramers-Kronig integral: $A'_{ij}(\omega) = \frac{2}{\pi} P \int_0^\infty [\zeta A''_{ij}(\zeta)/(\zeta^2 - \omega^2)] d\zeta$, where P denotes a principal-value integral. In nonequilibrium systems such as cells, however, both thermal and actively generated forces act on the probe particles. Here it is critical to combine AMR and PMR in the same experiment to separate active from thermal fluctuations [10]. AMR gives the material response A_{ij}, from which we can estimate the thermal part of the fluctuations $2k_B T A''_{ij}/\omega$ via the FDT. If thermal and nonthermal fluctuations are uncorrelated, the nonthermal fluctuation spectrum $P_{\mathrm{act}}(\omega)$ can then be determined as the difference between the total spectrum measured by PMR and the thermal spectrum estimated by AMR:

$$P_{\mathrm{act}}(\omega) = \langle u_i u_j^* \rangle - 2k_B T A''_{ij}/\omega. \quad (2)$$

This expression quantifies the extent of mechanical nonequilibrium in the system. The physical origin of $P_{\mathrm{act}}(\omega)$ depends on the system under investigation [23]. We proceed to calculate from $P_{\mathrm{act}}(\omega)$ the frequency dependence of the active traction forces that the cells exert on their environment, represented by the trapped particles.

Figure 1(b) shows the fluctuations in the measured forces $ku_1(t)$ and $ku_2(t)$ for each probe particle, where trap stiffness k was made equal in the two traps. The forces appear largely balanced, i.e., they add to zero, which suggests that intracellularly generated forces are predominant. For comparison, the same experiment was carried out with an actin-coated vesicle in equilibrium [Figs. 1(c) and 1(d)], where no such large and slow fluctuations were seen. The response function of a MLO-Y4 cell A_{12} measured directly by AMR is shown in Fig. 2, compared to the normalized fluctuation cross correlation $\omega\langle u_1 u_2^* \rangle / 2k_B T$ measured by PMR. At frequencies higher than 10 Hz, AMR and PMR agree, as if the system was in equilibrium. At lower frequencies, the PMR result shows a negative correlation while A_{12} measured by AMR shows predominantly elastic response. Below 10 Hz, the mechanical response of the cell is thus quasistatic [24], but the violation of the FDT shows that the system is out of equilibrium. Fluctuations here are dominated by the nonequilibrium cellular forces.

Having isolated the nonequilibrium fluctuations, we now analyze their spectral characteristics and speculate about the underlying cellular processes creating these fluctuations. Figure 3(a) shows that the power spectra of the transmitted force fluctuations, $-k^2\langle u_1 u_2^* \rangle$, approximately follow a scaling law $-k^2\langle u_1 u_2^* \rangle \sim \omega^{-2}$ with an amplitude that depends on the trap stiffness k. The spectral density at 0.19 Hz is plotted versus k in Fig. 3(b) and shows a monotonic increase with k for small trap stiffnesses, leveling off at high trap stiffnesses. This result, at first glance, appears to suggest that the cells generate more force when pulling against a stiffer trap. The simpler explanation is, however, that the internally generated forces both deform the cell itself and displace the particles in the traps, all of which can be modeled as coupled harmonic springs (Fig. 4). How the elastic energy is divided up between the cell and the traps depends on the relative stiffnesses. When the optical trap is weak, internally generated forces mainly deform the cell, but when the traps are stiff, forces are efficiently transmitted to the probe particles without deforming the cell. The optical traps assume the role of an

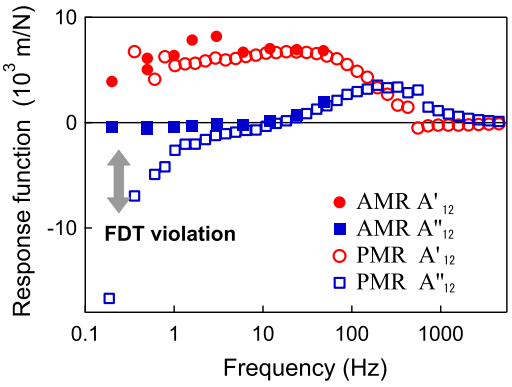

FIG. 2 (color online). A_{12} measured with AMR (filled symbols) compared to the normalized fluctuation power spectral density measured with PMR (open symbols). Circles and squares show real and imaginary parts, respectively.

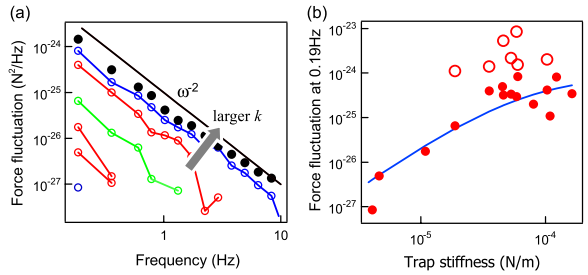

FIG. 3 (color online). (a) Frequency dependence of the (attenuated) force fluctuations detected by the particles $-k^2\langle u_1 u_2^*\rangle$. The power spectral density of the total fluctuating force $\langle FF^*\rangle$ (filled circles) follows an ω^{-2} power law. (b) Trap-stiffness dependence of the transmitted force fluctuations $-k^2\langle u_1 u_2^*\rangle$ at 0.19 Hz (filled circles) and of the total fluctuating force $\langle FF^*\rangle$ (open circles). The solid line is the fit of Eq. (3) to the data.

elastic environment usually provided by an extracellular matrix or neighboring cells, which can now be controlled by the trapping laser power.

To quantify these ideas, we model cell and traps as coupled springs (Fig. 4). Here, k_{12} denotes the effective elastic constant of the cell. Under balanced forces F and $-F$, the displacements of the probe particles are $u_1 = -u_2 = -F/(k + 2k_{12})$, giving

$$-k^2\langle u_1 u_2^*\rangle = \frac{k^2}{(k + 2k_{12})^2}\langle FF^*\rangle. \quad (3)$$

We obtained both cell stiffness (16 measurements with five different cells) $k_{12} = (3.8 \pm 2.1) \times 10^{-5}$ (N/m) and total cellular force generation $\langle FF^*\rangle$ (0.19 Hz) $= (1.4 \pm 1.0) \times 10^{-24}$ (N^2/Hz) by fitting Eq. (3) to the data. The resulting value for k_{12} is consistent with the value directly obtained from AMR (force-distance curve) [21,24].

In order to extend this model to a general frequency-dependent response, we consider the Langevin equation,

$$\int_{-\infty}^{t} \{\xi_{11}(t - t')\dot{u}_1(t') + \xi_{12}(t - t')\dot{u}_2(t')\}dt' = -ku_1 + K_1 + F_1, \quad (4)$$

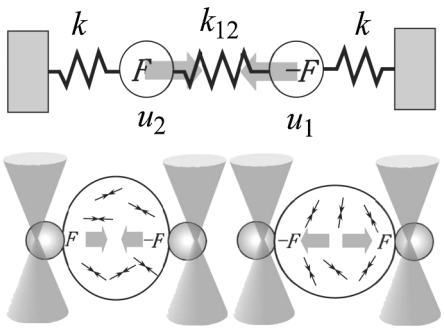

FIG. 4. Simple model of the mechanical components in our experimental configuration. k_{12} and k denote the stiffnesses of the cell and the optical traps, respectively, u_1, u_2 are the displacements of each particle. F denotes the total traction force as a sum of local forces as sketched in the lower panel.

and similarly for switched indices. Here, K_i is the thermally fluctuating force acting on particle i, and $F_2 = -F_1 = F$ is the total traction force between probe particles. It is important to take into account the fact that the particles feel both the viscoelastic response of the cell and the trap potentials. The drag coefficient tensor ξ_{ij} describes only the cell response. The random thermal force, however, is related via the FDT to the total drag coefficient tensor of the system, including the trap effects, $\gamma_{ij}(= 1/i\omega A_{ij})$ by $\langle K_i K_j^*\rangle = 2k_B T\,\mathrm{Re}[\gamma_{ij}]$. The cross-power spectrum is calculated via the Fourier transform of Eq. (4) as

$$P_{\mathrm{act}}(\omega) = -\langle FF^*\rangle(A_{11} - A_{12})(A_{22}^* - A_{12}^*). \quad (5)$$

Open circles in Fig. 3(b) show the total traction force obtained from this model which is not measurably influenced by trap stiffness. The force transmitted to the probe particles, on the other hand, does vary with trap stiffness and only at large k converges towards the total traction force. Note that comparing AMR and PMR in Eq. (4) lets us obtain the total traction force without making the assumptions used in Eq. (3). Equation (3) neglects thermal forces and assumes a quasistatic mechanical response, which was justified here merely because $A_{12}'' \approx 0$ at low frequencies (Fig. 2).

It remains to link the observed force fluctuations to microscopic molecular events in the cell. We here provide a simple scaling discussion. The generators of force are motor proteins acting within the cytoskeleton. Typically, bipolar aggregates of cytoplasmic myosins bridge F-actin filaments or bundles and generate contractile forces [25]. Since one can neglect external forces reaching into the cell, each such elementary force-generating unit can be modeled as an internally balanced force dipole [26]. We now derive an approximate expression for the displacement field u at a distance r from a single dipole in the low-frequency quasistatic limit where the elastic response of the cell dominates. Suppose the dipole consists of forces $\pm f$ separated by a distance ε. To leading order in ε, and for a linear elastic response, u must be proportional to $\varepsilon f/\mu$ with μ the shear modulus [27]. For the probe particles attached to opposing cell boundaries, the distance to the force generators is of order $r \sim R$. The only possible scaling form for u driven by a single intracellular dipole is then $u \sim \varepsilon f/\mu R^2$. The direction of the total force dipole is dependent on the average orientation of local force generators as shown in Fig. 4 (lower panel). Assuming, for the sake of simplicity, that the activities and directions of local dipoles are uncorrelated, their collective activity driven by N dipoles in the cell then gives a product $u^2 \sim N(\varepsilon f/\mu R^2)^2$. Inserting reasonable values for a cell ($\varepsilon \approx \mu$m, $f \approx$ pN, $\mu \approx 100$ Pa [21], $N \approx 1000$, and $2R \approx 10$ μm) results in $u^2 \sim 10^{-16}$ m^2. This estimate corresponds to the mean square displacement explored by the probe particles within ≈ 1 s [Fig. 1(b)]. Larger fluctuations on longer time scales are likely driven by the correlated activity of force dipoles which scales as

$u^2 \sim N^2(\varepsilon f/\mu R^2)^2 \sim 10^{-13}$ m^2, still consistent with our data [Fig. 1(b)].

The approximate $\langle FF^* \rangle \sim \omega^{-2}$ frequency dependence shown in Fig. 3(a) has also been widely seen with probe particles embedded in cells [16,28]. It has furthermore been observed in nonequilibrium model cytoskeletal networks activated by myosins [11]. The origin of this scaling behavior in the latter case appeared to be the occurrence of sudden force release events [11,29]. In our cell experiments such release events were not evident, leaving the case open for further inquiry. Note that it is easy to confuse the nonequilibrium fluctuations in viscoelastic cells with diffusion in a purely viscous environment which produces the same power law.

Cellular forces have been examined using atomic force microscopy or elastic substrates [7,30]. These techniques detect merely the force transmitted to the probes, which depends on substrate response even if total cellular force generation remains the same, as we have shown. This fact has been largely neglected. The uniqueness of our approach is the ability to measure ''total'' cellular force as well as transmitted force.

Cells exhibit threshold responses which points to a mechanism that compares internal and external stiffness. For fibroblasts it was found [31] that stress fibers (bundles of F-actin and myosin) are created only when the substrate elasticity is >3 kPa, which is comparable to the cell elasticity. Mesenchymal stem cells can even adapt their own rigidity to their environment [32]. The comparison between inside and outside elastic response could be very directly performed by a force sensor located at the cell membrane, e.g., at focal adhesion complexes [4,5], because, as we have shown here, the intracellularly generated force is only efficiently transmitted to the extracellular matrix when the stiffness of the surrounding matrix is larger than that of the cell itself.

Since mechanosensing is a crucial component of cell-cell and cell-tissue communication, understanding the physical mechanisms of these cellular sensory capabilities will be relevant both for understanding cell development and differentiation and for applications in tissue engineering.

We thank A. Lau and F. MacKintosh for helpful discussions and J. Klein-Nulend and T. Smit for supplying cell cultures. This work was supported by the Sonderforschungsbereich SFB755 of the German Research Foundation (DFG) and by the DFG Center for the Molecular Physiology of the Brain (CMPB). D. M. was further supported by KAKENHI, a Program for the Improvement of the Research Environment for Young Researchers from SCF (Japan).

[1] V. Vogel and M. Sheetz, Nat. Rev. Mol. Cell Biol. **7**, 265 (2006).
[2] D. E. Discher, P. Janmey, and Y. L. Wang, Science **310**, 1139 (2005).
[3] M. R. K. Mofrad and R. D. Kamm, *Cytoskeletal Mechanics: Models and Measurements* (Cambridge University Press, Cambridge, England, 2006).
[4] J. Y. Shyy and S. Chien, Circ. Res. **91**, 769 (2002).
[5] H. B. Wang *et al.*, Proc. Natl. Acad. Sci. U.S.A. **98**, 11 295 (2001).
[6] B. Geiger *et al.*, Nat. Rev. Mol. Cell Biol. **2**, 793 (2001).
[7] N. Q. Balaban *et al.*, Nat. Cell Biol. **3**, 466 (2001).
[8] L. A. Hough and H. D. Ou-Yang, Phys. Rev. E **65**, 021906 (2002).
[9] D. Mizuno, Y. Kimura, and R. Hayakawa, Phys. Rev. Lett. **87**, 088104 (2001).
[10] D. Mizuno, D. A. Head, F. C. MacKintosh, and C. F. Schmidt, Macromolecules **41**, 7194 (2008).
[11] D. Mizuno *et al.*, Science **315**, 370 (2007).
[12] T. G. Mason and D. A. Weitz, Phys. Rev. Lett. **74**, 1250 (1995).
[13] B. Schnurr, F. Gittes, F. C. MacKintosh, and C. F. Schmidt, Macromolecules **30**, 7781 (1997).
[14] F. Gittes, B. Schnurr, P. D. Olmsted, F. C. MacKintosh, and C. F. Schmidt, Phys. Rev. Lett. **79**, 3286 (1997).
[15] M. Buchanan *et al.*, Macromolecules **38**, 8840 (2005).
[16] A. W. C. Lau, B. D. Hoffmann, A. Davies, J. C. Crocker, and T. C. Lubensky, Phys. Rev. Lett. **91**, 198101 (2003).
[17] S. C. Cowin, L. Mosssalentijn, and M. L. Moss, J. Biomech. Eng. **113**, 191 (1991).
[18] F. Gittes and C. F. Schmidt, Opt. Lett. **23**, 7 (1998).
[19] M. W. Allersma *et al.*, Biophys. J. **74**, 1074 (1998).
[20] F. Gittes and C. F. Schmidt, Methods Cell Biol. **55**, 129 (1997).
[21] R. G. Bacabac *et al.*, J. Biomech. **41**, 1590 (2008).
[22] E. Helfer *et al.*, Phys. Rev. E **63**, 021904 (2001).
[23] T. Harada and S. I. Sasa, Phys. Rev. Lett. **95**, 130602 (2005).
[24] The response of the cells corresponds to a shear modulus of $\sim$100 Pa. The frequency dependence was consistent with the widely observed weak power-law behavior at low frequencies as well as $\omega^{3/4}$ scaling, typical for cytoskeletal polymers, at high frequencies; see EPAPS Document No. E-PRLTAO-102-034917 for supplementary information discussing the high bandwidth rheological property of cells measured with our two-particle assay. For more information on EPAPS, see http://www.aip.org/pubservs/epaps.html.
[25] D. P. Kiehart and R. Feghali, J. Cell Biol. **103**, 1517 (1986).
[26] Y. Hatwalne, S. Ramaswamy, M. Rao, and R. A. Simha, Phys. Rev. Lett. **92**, 118101 (2004).
[27] L. D. Landau and E. M. Lifshitz, *Theory of Elasticity* (Pergamon, Oxford, 1986), 3rd ed.
[28] P. Bursac *et al.*, Biochem. Biophys. Res. Commun. **355**, 324 (2007).
[29] F. C. MacKintosh and A. J. Levine, Phys. Rev. Lett. **100**, 018104 (2008).
[30] M. Prass *et al.*, J. Cell Biol. **174**, 767 (2006).
[31] T. Yeung *et al.*, Cell Motil. Cytoskeleton **60**, 24 (2005).
[32] A. J. Engler *et al.*, Cell **126**, 677 (2006).